

MODELING AND SIMULATION OF A PWM RECTIFIER INVERTER INDUCTION MOTOR DRIVE SYSTEM IMPLEMENTING SPEED SENSOR LESS DIRECT VECTOR CONTROL

Salam Ibrahim Khather
 Design Engineer
 Elec. Eng. Dept.
 KAR Company
 Iraq

Email: salam_asmer@yahoo.com, saias.eleeng@yahoo.com

ABSTRACT

The paper describes control method for PWM rectifier- inverter induction motor drive. A control scheme is developed that uses stator flux oriented direct vector control (voltage source current controlled PWM inverter) for the induction motor and voltage source voltage controlled PWM rectifier to special configurations for harmonic reduction and unity power factor operation.

Keywords

PWM Rectifier- Inverter system, Adjustable speed sensor less drive for induction machine, Stator flux oriented direct vector control.

1. INTRODUCTION

Vector control schemes without a speed sensor are the most suitable solution in applications where a combination of good performance characteristics and low cost is required [1].

A modern adjustable speed ac machine system is equipped with an adjustable frequency drive (AFD). The AFD is a power electronic device for torque and speed control of an electric machine. The AFD controls the torque and speed of the electric machine by converting the fixed voltage and frequency of the grid to adjustable values on the machine side. An AFD converter for an electric machine can be designed with various power electronic principles. The six pulse diode rectifier and pulse width modulated (PWM) inverter with an intermediate voltage stiff direct voltage link is

perhaps the most widespread AFD technology in industrial applications. The six pulse diode rectifier and PWM inverter is a cost-effective and high-efficiency AFD that is hard to beat. However, alternative PWM rectifier- inverter topologies can be attractive in certain applications since the six pulse diode rectifier and PWM inverter only permits one power flow direction and injects low order current harmonics to the grid.

The PWM rectifier-inverter Fig. (1) that uses PWM converters on both the grid and machine side is one such alternative converter topology. The PWM rectifier-inverter offers a bi-directional power flow, full control of the direct voltage and the grid current, and reduced grid current distortion [2, 3].

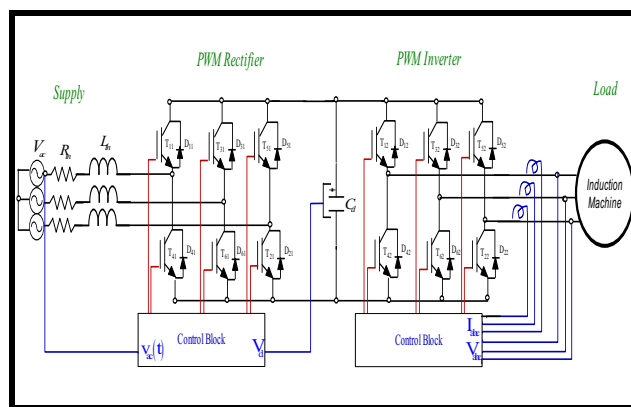


Fig. (1) The PWM rectifier-inverter drive system.

2. VOLTAGE SOURCE VOLTAGE CONTROLLED PWM RECTIFIER

Fig. (2) Shows a voltage-source voltage-controlled rectifier is derived.

This diagram represents an equivalent circuit of the fundamentals, that is, pure sinusoidal at the mains side, and pure dc at the dc link side [4]. The control is achieved by creating a sinusoidal voltage template v_{MOD} , which is modified in amplitude and angle to interact with the mains voltage $v_{ac}(t)$. In this way the input currents are controlled without measuring them. The template v_{MOD} is generated using the differential equations that govern the rectifier. The following differential equation can be derived:

$$v_{ac}(t) = \sqrt{2}V_{ac} \sin \omega t \quad \dots (1)$$

$$i_s(t) = I_{MAX}(t) \sin(\omega t + \theta_s) \quad \dots (2)$$

$$v_{ac}(t) = L_{in} \frac{di_s}{dt} + R_{in} i_s + v_{MOD}(t) \quad \dots (3)$$

Equations (1), (2) and (3) allow a function of time able to modify v_{MOD} in amplitude and phase that will make the rectifier work at a fixed power factor. Combining these equations with (1) yields:

$$v_{MOD}(t) = [\sqrt{2} V_{ac} + X_{in} I_{MAX} \sin \theta_s - (R_{in} I_{MAX} + L_{in} \frac{dI_{MAX}}{dt}) \cos \theta_s] \sin \omega t - [X_{in} I_{MAX} \cos \theta_s + (R_{in} I_{MAX} + L_{in} \frac{dI_{MAX}}{dt}) \sin \theta_s] \cos \omega t. (4)$$

Equation (4) provides a template for v_{MOD} , which is controlled through variations of the input current amplitude I_{MAX} . The derivatives of I_{MAX} into Equ. (4) make sense, because I_{MAX} a change every time the dc load is modified.

This equation can also be written for unity power factor operation as:

$$v_{MOD}(t) = [\sqrt{2} V_{ac} - R_{in} I_{MAX} - L_{in} \frac{dI_{MAX}}{dt}] \sin \omega t - [X_{in} I_{MAX}] \cos \omega t \quad \dots (5)$$

With this last equation, a unity power factor, voltage source, voltage controlled PWM

rectifier can be implemented as shown in Fig. (2) It can be observed that Equ. (4) and (5) have an in-phase term with the mains supply $\sin \omega t$, and an in-quadrature term $\cos \omega t$. These two terms allow the template v_{MOD} to change in magnitude and phase so as to have full unity power factor control of the rectifier.

In this control block no need to sense the input currents. However, to ensure stability limits as good as the limits of the current-controlled rectifier, blocks $-R_{in} - SL_{in}$ and $-X_{in}$ in Fig. (2) have to emulate and reproduce exactly the real values of R_{in} , X_{in} and L_{in} of the power circuit. However, these parameters do not remain constant, and this fact affects the stability of this system if the impedance parameters are reproduced exactly [5].

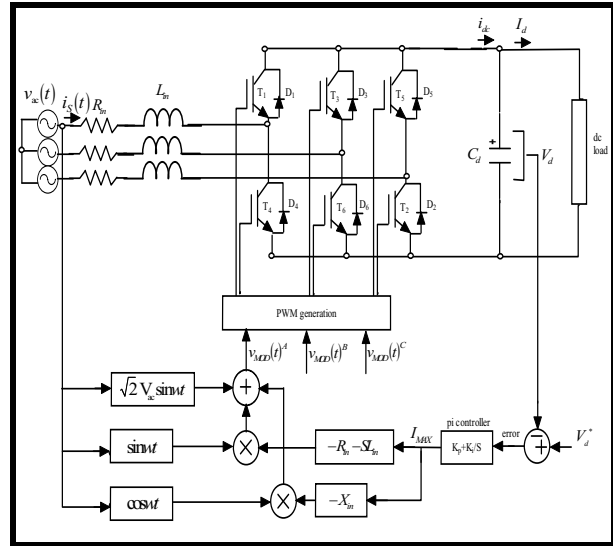


Fig. (2) Implementing of the voltage-controlled rectifier unity power factor operation.

3. STATOR FLUX ORIENTED DIRECT VECTOR CONTROL

Stator flux oriented direct vector control has the advantage that flux vector estimation accuracy is affected by the stator resistance variation only [6].

We will develop a strategy for Stator flux oriented direct vector control by manipulating equation derived from $d^e - q^e$ equivalent circuit. The control block diagram at Stator flux oriented direct vector control is shown in figure (3).

The key estimation equation can be summarized as follows:

$$\psi_{qs}^s = \int (v_{qs}^s - R_s i_{qs}^s) dt \quad . (6)$$

$$\psi_{ds}^s = \int (v_{ds}^s - R_s i_{ds}^s) dt \quad . (7)$$

$$\hat{\psi}_s = \sqrt{(\psi_{qs}^s)^2 + (\psi_{ds}^s)^2} \quad . (8)$$

$$\sin \theta_e = \frac{\psi_{qs}^s}{\hat{\psi}_s} \quad . (9)$$

$$\cos \theta_e = \frac{\psi_{ds}^s}{\hat{\psi}_s} \quad . (10)$$

$$i_{dq} = \frac{\sigma \tau_r \omega_{sl} i_{qs}}{(1 + \sigma S \tau_r)} \quad . (11)$$

Where vector $\hat{\psi}_s$ is represented by magnitude of ψ_s . Signals $\cos \theta_e$ and $\sin \theta_e$ have been plotted in correct phase position in fig(3b). These unit vector signals give arid of current i_{ds} on the d^e -axis (direction of $\hat{\psi}_s$) and current i_{qs} on the q^e -axis as shown. At this condition $\psi_{qs} = 0$ and $\psi_{ds} = \hat{\psi}_s$ as indicated in the phasor diagram of fig (3a).when the i_{qs} polarity is reversed by the speed loop, the i_{qs} position in fig (3a) also reverses, giving negative torque. The generation of a unit vector signal from feedback flux vector gives the name (direct vector control) [7].

Where i_{dq} is the decoupling compensation current, and all others are standard symbols. The

advantage of stator flux orientation is that it has less parameter variation effect [8].

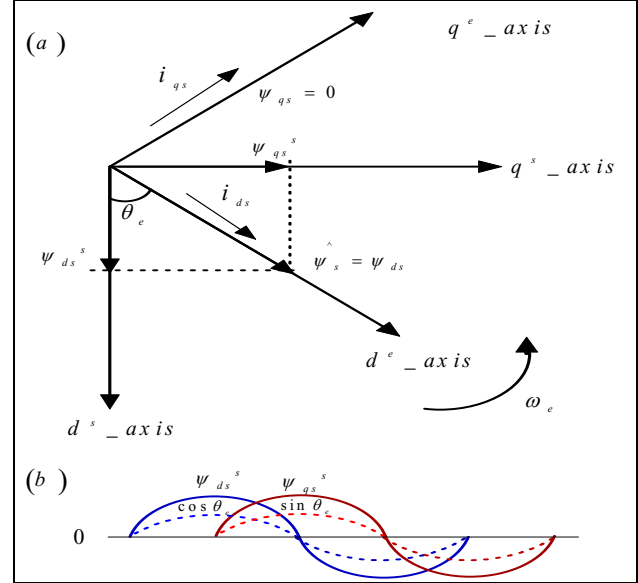


Figure (3): (a) $d^s - q^s$ and $d^e - q^e$ phasor showing correct stator flux orientation.

(b) Plot of unit vector signals in correct phase position.

The estimation equations are only sensitive to stator resistance variation which is somewhat easy to correct. The variation of stator leakage inductance, rotor leakage inductance and magnetizing inductance does not contribute to flux estimation error. The main demerit for stator flux orientation is the coupling effect and the corresponding decoupling compensation needed in the stator flux loop [9]. The decoupling current i_{dq} is a function of i_{qs} , i_{ds} and ψ_{ds} , and is dependent on the stator inductance parameters. Note that this parameter dependence has only a small effect on the transient response, but has no effect on the static response [7].

4. SPEED ESTIMATION METHOD

Speed can be calculated from slip frequency ω_{sl} from the relation $\omega_r = \omega_e - \omega_{sl}$, where

ω_e =stator frequency (rad/sec). The ω_{sl} signal was calculated before in stator flux oriented direct vector control as:

$$\omega_{sl} = \frac{(1 + \sigma S \tau_r) L_s i_{qs}}{\tau_r (\psi_{ds} - \sigma L_s i_{ds})} \quad (12)$$

Where $\sigma = 1 - L_m^2 / L_s L_r$, $T_r = L_r / R_r$ and

i_{ds} , i_{qs} and ψ_{ds} are the signal corresponding to stator flux orientation.

The expression for stator frequency is given as [7]:

$$\omega_e = \frac{d\theta_e}{dt} = \frac{(v_{qs}^s - i_{qs}^s R_s) \psi_{ds}^s - (v_{ds}^s - i_{ds}^s R_s) \psi_{qs}^s}{\psi_s^2} \quad (13)$$

5. INDUCTION MOTOR MODEL

Fig(4) shows the d-q equivalent circuits for a three phase symmetrical squirrel cage induction motor in synchronously rotating frame with zero sequence component neglected [10,11,12]. From the dynamic equivalent circuit, the induction motor parameters can be expressed in matrix equation (14); assuming that the rotor bars in squirrel cage induction motor are shorted out and the rotor voltages equal zero [1].

$$\begin{bmatrix} v_{qs} \\ v_{ds} \\ 0 \\ 0 \end{bmatrix} = \begin{bmatrix} R_s + S L_s & \omega_e L_s & S L_m & \omega_e L_m \\ -\omega_e L_s & R_s + S L_s & -\omega_e L_m & S L_m \\ S L_m & (\omega_e - \omega_r) L_m & R_r + S L_r & (\omega_e - \omega_r) L_r \\ -(\omega_e - \omega_r) L_m & S L_m & -(\omega_e - \omega_r) L_r & R_r + S L_r \end{bmatrix} \begin{bmatrix} i_{qs} \\ i_{ds} \\ i_{qr} \\ i_{dr} \end{bmatrix} \quad (14)$$

Where R_s , R_r are the stator and rotor resistance per phase respectively, L_s , L_r are the stator, and the rotor inductance per phase, respectively,

$S = \frac{d}{dt}$ operator, ω_e, ω_r are synchronous and rotor speeds respectively.

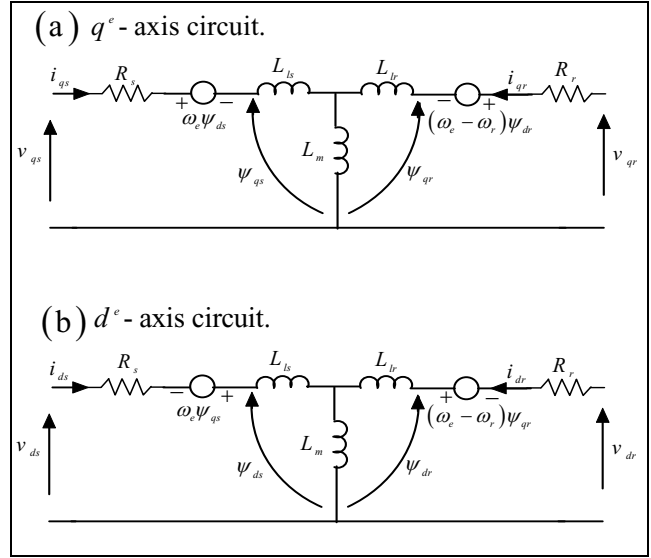


Fig (4) Dynamic equivalent circuit for induction motor.

6. SIMULATION STUDY

The block diagram of the proposed control strategy was simulated using MATLAB – SIMULINK as show in Fig (5).

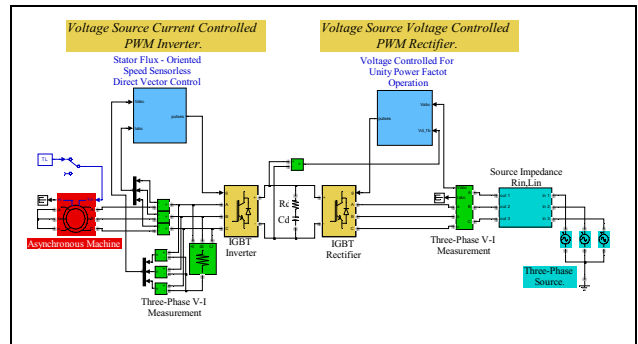


Fig (5). The block diagram of the PWM rectifier- inverter induction motor drive system.

The induction motor name plate parameters are given as 1.1 kW, 380V, 50Hz, 3.7A, 1360 rpm and simulated with dynamic d-q model using the nominal parameter as given in table (1).

At the following figures the simulation results during a speed reversing from 1360 rpm to -1360 rpm. The speed reversed is obtained with torque control 8 N.m as fan.

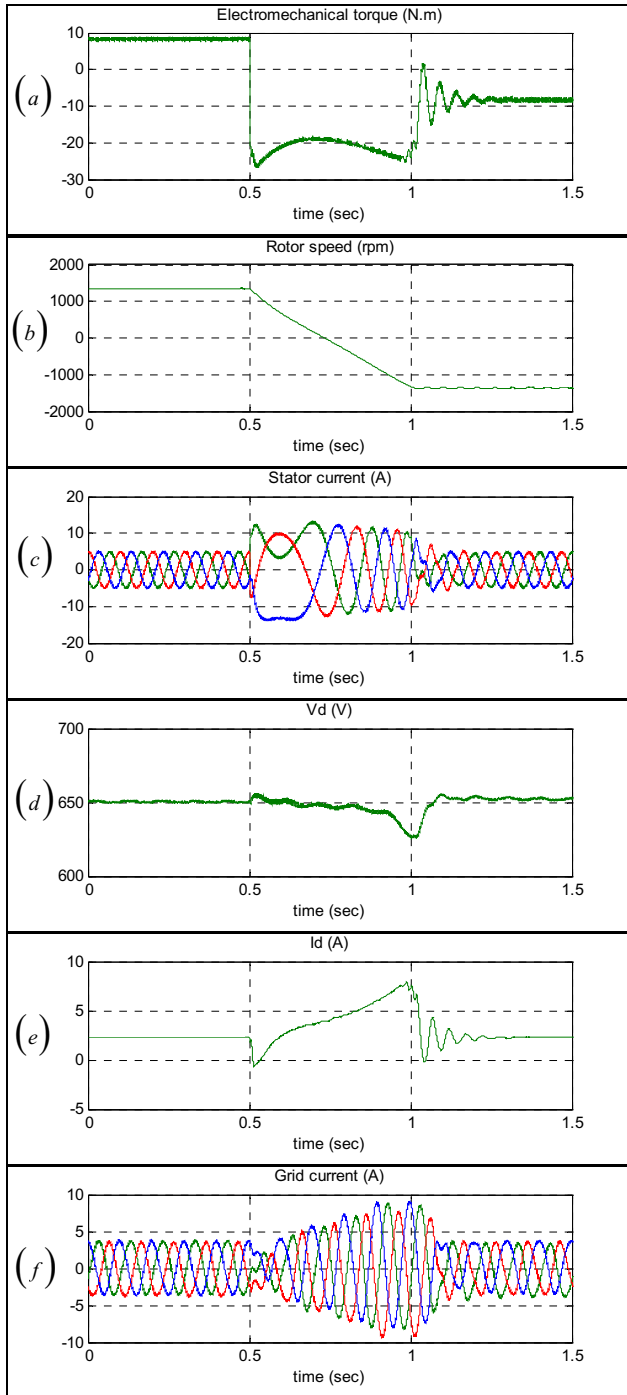


Fig (6). the simulation results: (a) The machine terminal phases current.(b) Electromechanical torque. (c) The motor speed.(d) Direct voltage.(e) Direct current. (f) Grid current.

Table (1) Machine parameters	
R_s	5.1 (Ω)
R_r	6.7 (Ω)
L_{ls}	16.7 (mH)
L_{lr}	16.7 (mH)
L_m	251 (mH)

We are using the hysteresis band current controller PWM with hysteresis band of 0.5 A [13].

The speed control is possible in four quadrants without any additional control element. In motor braking condition, the torque T_e is negative; the drive initially goes into regenerative braking mode.

The grid side power factor is 0.9 lagging and total harmonics distortion is 6%.

7. CONCLUSION

The paper demonstrates a speed sensorless stator flux oriented direct vector control in an induction machine drive system. Simulation tests verify the performance of four quadrant induction machine drive system and power line condition for sinusoidal current and power factor correction. The proposed control method assures:

- Torque and stator flux have been controlled nearly independently.
- High dynamics of speed control.
- Good stabilization of load torque for wide range speed control.
- Regenerative braking.
- Low THD.
- PF correction.

8. REFERENCES

- [1] Bimal K. Bose., "Neural Network Applications in Power Electronics and Motor Drives an Introduction and Perspective "IEEE Transactions On Industrial Electronics, Volume 54, NO. 1, FEBRUARY 2007.
- [2] ROLF OTTERSTEN"Vector Control of a Double-Sided PWM Converter and Induction Machine Drive"SE-412 96 GÄoteborg,Sweden 2000.
- [3] Salam Ibrahim Khather "Modeling and Simulation of a PWM Rectifier-Inverter Induction Machine Drive System Without Speed Sensor" M.SC. thesis,Iraq, 2008.
- [4] Muhammad H. Rashid., "Power Electronics Handbook" Academic Press. ISBN 0-12-581650-2, Chapter26, Yahya Shakweh., "Drive Types and Specifications", 2001.
- [5] Muhammad H. Rashid., " Power Electronics Handbook" Academic Press. ISBN 0-12-581650-2, Chapter12, Juan W. Dixon., " Three-Phase Controlled Rectifiers", 2001.
- [6] Epaminondas D. Mitronikas and Athanasios N. Safacas.,"An Improved Sensorless Vector-Control Method for an Induction Motor Drive" IEEE Transactions on Industrial Electronics, Volume 52, NO. 6, DECEMBER 2005.
- [7] Bimal K. Bose. "Modern Power Electronic and AC Drive" Prentice Hall PTR, ISBN 0-13-016743-6, 2002.
- [8] Xingyi Xu, and Donald W. Novotny., " Selection of the Flux Reference for Induction Machine Drives in the Field Weakening Region" IEEE Transactions on Industry Applications, Volume 28, no. 6, November / December 1992.
- [9] Dr. Dhiya Ali Al-Nimma and Salam Ibrahim Khather "Modeling and simulation of a speed sensorless vector controlled induction motor drive system" IEEE CCECE Page(s):27 – 32, 2011.
- [10] Marek Jasinski, Marian P.Kazmierkowski., "Direct Power Constant Switching Frequency Control of AC/DC/AC Converter-Fed Induction Motor" Industrial Technology, IEEE International Conference on Industrial Technology (ICIT), Volume 2, 8-10 Dec, Page(s):611 – 616, 2004.
- [11] M.Jasinski and M.P.Kazmierkowski., "Sensorless Direct Power and Torque Control of PWM Back-To-Back Converter-Fed Induction Motor" The 30th Annual Conference of the IEEE Industrial Electronics Society, Volume 3, 2-6 Nov, Page(s):2273 – 2278, 2004.
- [12] Anitha Paladugu and Badrul H. Chowdhury., "Sensorless Control of Inverter-Fed Induction Motor Drives" Electric Power Systems, Volume 77, Issues 5-6, April, and Pages: 619-629, Elsevier 2007.
- [13] S.R Bowes and D. Holliday.," Comparison of Pulse-Width-Modulation Control Strategies For Three-Phase Inverter Systems" IEE Proc. Electr. Power Appl., Volume 153, No. 4, July 2006.